Dalton Transactions

Accepted Manuscript

ROYAL SOCIETY OF CHEMISTRY

www.rsc.org/dalton

Journal Name

ARTICLE

Fabrication of nano-drug delivery system based layered rare-earth hydroxides integrating drug-loading and fluorescence properties

Received 00th January 20xx,
Accepted 00th January 20xx

DOI: 10.1039/x0xx00000x

www.rsc.org/

Qingyang Gu,* Wen Chen, Fei Duan, Ruijun Ju

We demonstrate the first example of intercalation naproxen (abbr. NPX) into layered europium hydroxide (LEuH) and investigate the structure, chemical composition, thermostability, morphology, luminescence property, cytotoxic effect, and controlled-release behaviors. Different deprotonation degree leads to NPX-LEuH composites with diverse structure (horizontal or vertical arrangement), and the thermal stability of organics is enhanced after intercalation. The Eu^{3+} luminescence in NPX-LEuH composites is enhanced, especially for the NPX-LEuH-1:0.5 composite. The content of naproxen in the intercalation material can be confirmed by HPLC. The cytotoxic effect of LEuH is observed with a sulforhodamine B (SRB) colorimetric assay, which reveal that the LEuH has low cytotoxic effects on most cells. In addition, the NPX-LEuH nanocomposites can control the release of NPX in Na_2HPO_4-NaH_2PO_4 buffer solution at pH 6.86 and 37°C, and the complete release needs about 200 min. The release mechanism can be ascribed to the ion-exchange reaction between NPX and $HPO_4^{2-}/H_2PO_4^-$ in bulk solution. The ion-exchange velocity is fast at beginning and slows down gradually with the exchange reaction. The construction of LRHs composites with drug molecules provides a beneficial pathway for preparing nano-drug delivery system based LRHs integrating drug-loading and fluorescence properties.

1. Introduction

In recent years, increasing attention has been directed to the investigation of inorganic drug delivery systems for safe drug delivery. Inorganic drug delivery systems can allow safe and controlled delivery of various bioagents into targets with high efficiency.[1] Both natural and synthetic materials have been tested and proposed as components of new drug delivery systems (NDDS) and many efforts have been made to synthesise materials with the biological, technological, and mechanical properties for each application in drug delivery. [2, 3] In recent years, many types of materials including inorganic silica,[4, 5] carbon materials,[6, 7] and polymeric matrix[8, 9] have been employed as substrates for drug delivery. Among a variety of inorganic materials, layered materials have attracted intense interest because of the rich interlayer chemistry.[10] The intercalation of guests into inorganic hosts can influence the properties of both the host layers and gallery guests, especially enhance the chemical, thermal and photolytic stability of the guests because of a protective environment provided by host layer.[11] Layered double hydroxides (LDHs), as an anionic type layered material, has shown great promises for the delivery of chemical therapeutics and bioactive molecules to mammalian cells in vitro and in vivo. This system offers high efficiency and drug loading density, as well as excellent protection of loaded molecules from undesired degradation.[12] The cationic layered framework of LDHs leads to safe accommodation of many biologically important molecules including genes or drugs.[13, 14] Toxicological studies have also found LDHs to be biocompatible compared with other widely used nanoparticles, such as iron oxide, silica, and single-walled carbon nanotubes. A plethora of bio-molecules have been reported to either attach to the surface or intercalate into LDHs materials through co-precipitation or anion-exchange reaction, including amino acid, peptides, vitamins, and polysaccharides, etc.[12]

Layered rare-earth hydroxides (LRHs) with a general formula of $[RE_2(OH)_5(H_2O)_n][A^{m-}]_{1/m}$ (RE = rare-earth cations, A^{m-} = anions),[15] as one kind of layered materials with positive layers, have been extensively studied due to their applications as catalysts,[16, 17] adsorbent,[18] and optical materials.[19-21] Concerning intercalation of LRHs, most of the reports described their anion exchange behaviors and luminescence properties, while there have been lack of studies focusing on drug delivery, except our published work concerning the intercalation of amino acids into Eu^{3+}-doped layered gadolinium hydroxide(LGdH:Eu) and take advantage of the luminescence quenching effect to obtain luminescence probe to detect certain amino acids in biologic system.

Naproxen(abbr. NPX), (+)-(S)-2-(6-methoxynaphthalene-2-yl) propanoic, is a non-steroidal anti-inflammatory drug frequently used for the reduction of severe pain, fever, inflammation and stiffness caused by conditions such as osteoarthritis, rheumatoid arthritis, psoriatic arthritis, gout, tendonitis, and the treatment of primary dysmenorrhea.[22] In order for drug therapy

†Department of Chemical Engineering, Beijing Institute of Petrochemical Technology, Beijing 102617, China

Fax: 86 10 81292133; Tel: 86 10 81292133; E-mail: guqingyang@bipt.edu.cn

to be most effective, the desired pharmacological response must be obtained at the target without harmful interactions at other sites,[23] which requires controlled and correct drug dosage. The binding of drug molecules and rare earth ions can detect drug molecules sensitively by monitoring the luminescence change. In previous researches, the intercalation of NPX into LDHs and the controlled release behaviors have been studied, [24, 25] but there are no reports about the intercalation of NPX into LRHs and taking advangtage of the luminescence properties to detect drug molecules.

Herein we intercalate NPX into LEuH to form composites. The luminescence investigation shows that the incorporation of NPX with the LRH layer can sharply enhance the Eu^{3+} luminescence. This method can be applied as luminescence probe to detect NPX in biologic system. In addition, the NPX-LEuH nanocomposites can control the release of NPX, which can be used for nano-drug delivery system.

2. Experimental section

2.1 Preparation of NO_3–LEuH precursor.

The NO_3^- type LEuH (NO_3–LEuH) was synthesized *via* hydrothermal method as previously reported.[19, 26] An aqueous solution containing $Eu(NO_3)_3{\cdot}6H_2O$ (1 mmol), hexamethylenetetramine (HMT, 1 mmol), $NaNO_3$ (13 mmol), in deionized water (80 mL) was heated at 90 °C for 12 h in a Teflon-autoclave. After the reaction, the product was filtered, washed, and vacuum-dried (40 °C for 24 h), obtaining the NO_3–LEuH precipitate.

2.2 Intercalation of NPX into LEuH by ion exchange method.

The ion-exchange reactions between NO_3^- and the organic anions were processed at 70 °C in a Teflon-autoclave. Firstly, 1.26 mmol of NPX and 0.63 / 0.88 / 1.26 / 1.51 mmol of NaOH (corresponding to 1:0.5/1:0.7/1:1/1:1.2 molar ratio of NaOH to NPX) were mixed to the obtained solutions (80 ml). The NO_3–LEuH powder (~ 0.1 g) was dispersed into the above solutions, then reacted at 70 °C for 24 h in a Teflon-autoclave. The resulting precipitates were collected by filtration, washed with deionized water, and vacuum-dried at 40 °C for 24 h. The as-prepared composites are noted as NPX-LEuH-1:x, in which *x* is the molar ratio of NaOH to NPX, for example NPX-LEuH-1:0.5 represents the molar ratio of NaOH to NPX is 1:0.5.

2.3 Measurement of release amount of NPX.

Firstly, NPX-Na solution (2.0×10^{-5} mol·L^{-1}) was prepared by dissolving 0.2 mmol of NPX and 0.2 mmol of NaOH in 100 mL/0.025 mol·L^{-1} $NaHPO_4$-NaH_2PO_4 buffer solutions (pH=6.86). The absorbance peaks of NPX-Na were got by ultraviolet scanning. Secondly, the standard curve of concentration-absorbance of NPX-Na was obtained at the maximal absorption band (330 nm), and the testing concentration was 1.0×10^{-5}, 2.0×10^{-5}, 2.5×10^{-5}, 5.0×10^{-5} mol·L^{-1}, respectively. Finally, the release kinetic curve of NPX from NPX-LEuH was obtained in $NaHPO_4$-NaH_2PO_4 buffer solutions at pH 6.86 and 37°C.

2.4 Characterization Techniques.

The powder X-ray diffraction (XRD) patterns were collected by using a Phillips X'pert Pro MPD diffractometer with Cu-Kα radiation at room temperature, with a step size of 0.0167°, scan time of 15 seconds per step, and 2ϑ ranging from 4.5 to 70 °. The generator setting was 40 kV and 40 mA. For the small degrees, the XRD patterns were measured at room temperature with step size of 0.008 °, scan time of 30 seconds per step. Fourier transformed infrared (FT–IR) spectra of the samples were recorded on a Nicolet-360 Fourier-Transform infrared spectrometer by the KBr method. Scanning electron microscope (SEM) observations were carried out by using a Hitachi S-4800 microscope at 5.0 kV. Thermo-gravimetric and differential thermal analysis (TG-DTA) measurements were performed with a ZRY-2P thermal analyzer in air atmosphere. Luminescence spectra were obtained on Hitachi F-4500 spectrofluorimeter.

The metal ion contents were determined by inductively coupled plasma atomic emission spectroscopy (ICP-AES, Jarrel-ASH, ICAP-9000) after the solid products were dissolved in a 0.1 M HNO_3. C, H and N contents were determined by using an Elementar vario EL elemental analyzer. The chemical formula of the products were determined based on the results of ICP and CHN analyses.

The content of naproxen in the intercalation material was measured by HPLC (Agilent 1260 liquid chromatographic system, Agilent Technologies Inc., USA) with a Nucleodur 100-5 C18 column (250 × 4.6mm, 5.0 μm). The detection wavelength was set at 230 nm, and the analysis was performed at ambient temperature. The mobile phase consisted of acetonitrile, 0.02 M K_2HPO_3 and triethylamine (60:40:0.3, v/v/v). The pH was adjusted to 4.0 with phosphoric acid, and the flow rate was 1.0 ml/min.

To evaluate the cytotoxic effect of (NO_3-LEuH), brain glioma U87MG cells, breast cancer MDA-MB-435S cells, murine brain microvascular endothelial cells (BMVECs), and human umbilical vein endothelial cells (HUVECs) were seeded at a density of 6×10^3 cells/well in 96-well culture plates and cultured for 24 h. The cells were then treated with NO_3-LEuH in the range of 0 – 100.0 μg/ml. After incubation for another 48 h, the cytotoxic effect was observed with a sulforhodamine B (SRB) colorimetric assay. Briefly, the culture medium was discarded, and then the cells were fixed with trichloroacetic acid, followed by staining with SRB. Absorbance values were measured at 540 nm using a microplate reader (Tecan Infinite F50, Tecan Group Ltd. Switzerland).

3. Results and Discussion

3.1 Structure analyses of the as-prepared composites.

Fig. 1 shows the XRD patterns of the precursor and the formed composites. For NO_3–LEuH (Fig. 1a), a series of strong (00*l*) reflections at 0.83, 0.42 and 0.27 nm observed are characteristics of a layered phase, showing a basal spacing (d_{basal}) of 0.83 nm identical to the previously reported values.[19, 26] The sharp and symmetric diffraction peaks indicate a high

crystallinity. Fig. 1b shows the XRD pattern of the NPX-LEuH-1:0.5 composite prepared by ion-exchange method. It has two d_{basal} values of 2.23 and 1.50 nm, with series of (00*l*) reflections at 2.23, 0.97, 0.76, 0.58 nm and 1.50, 0.76, 0.51, 0.39 nm, respectively. For the composite of NPX-LEuH-1:0.7 (Fig. 1c), the d_{basal} value is 2.32, with series of (00*l*) reflections at 2.32, 1.17, 0.78, 0.58, 0.47, and 0.40 nm. When the molar ratio of NaOH and NPX is 1:1 and 1:1.2 (Fig. 1d, e), there is no reflection peak in the range of small angle，and the d_{basal} value is 0.76/0.75 nm. The 0.32 nm peak comes from the non-basal (220) reflection that represents the feature of the host layer,[27] and it does not change after ion-exchange, which shows the invariability of the host layer.

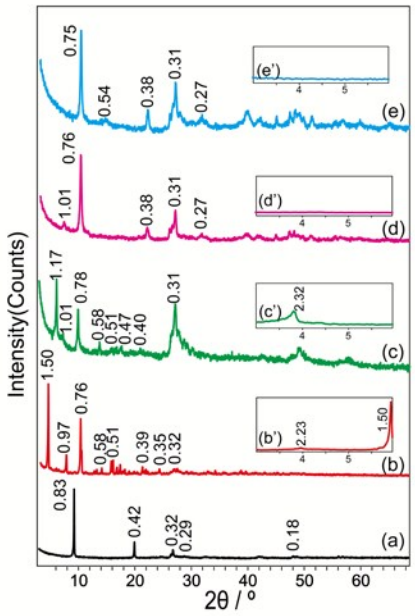

Fig. 1 XRD patterns of NO_3-LEuH (a) and composites of NPX-LEuH-1:0.5 (b,b'), NPX-LEuH-1:0.7 (c,c'), NPX-LEuH-1:1 (d,d'), NPX-LEuH-1:1.2 (e,e'). The *d*-values are given in nanometers.

For the NPX-LEuH-1:0.5 composite, on the basis of the layer thickness of LRHs (0.65 nm),[19] there exists two gallery heights, ca. 1.58 nm (= 2.23-0.65) and 0.85 nm (= 1.50-0.65). This may correspond to two kinds of arrangement structures of a monolayered vertical arrangement and a horizontal arrangement (Scheme 1b), considering that the NPX size of ca. 1.18×0.50×0.41 nm^3. This may be caused by the partial deprotonation. The NPX-LEuH-1:0.7 composite may correspond to a monolayered vertical arrangement (Scheme 1c). The organic guests strongly interact with each other via π-π interactions of naphthalene rings. The basal spacing of the composites of NPX-LEuH-1:1 and NPX-LEuH-1:1.2 is around 0.75 nm, which may be ascribed to the OH^- intercalated in the layers (Scheme 1d).

Based on ICP, CHN analyses and charge balance considerations, the estimated compositions of the LEuH precursor and the as-prepared composites are shown in Table 1. The presence of CO_3^{2-} may arise from HMT decomposition.[28, 29] For the composites of NPX-LEuH-1:0.5/0.7, almost half NPX neutral molecules exist in the compositions apart from partial deprotonated organics. The ratio of the deprotonated and the neutral NPX is agree with the amount of added NaOH. For the composites of NPX-LEuH-1:1/1.2, the excessive OH^- are intercalated into LEuH and the content of organics is little. This results are in agreement with the XRD patterns.

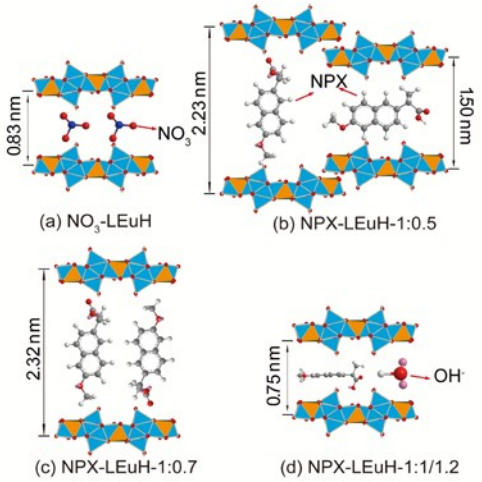

Scheme 1. Schematic representation of the proposed arrangement of the gallery species between the layers.

Table 1. Chemical compositions for LEuH: precursor and the composites.

Samples	Chemical formula	Wt %, Found			
		Eu	C	H	N
NO_3–LEuH	$Eu(OH)_{2.50}(NO_3)_{0.34}(CO_3)_{0.08}\cdot 0.69H_2O$	64.14	0.25	1.63	2.01
NPX-LEuH-1:0.5	$Eu(OH)_{2.50}(NO_3)_{0.02}(C_{14}H_{13}O_3)_{0.48}(C_{14}H_{14}O_3)_{0.51}\cdot 0.47H_2O$	45.13	49.44	4.26	0.10
NPX-LEuH-1:0.7	$Eu(OH)_{2.50}(CO_3)_{0.08}(C_{14}H_{13}O_3)_{0.34}(C_{14}H_{14}O_3)_{0.09}\cdot 0.07H_2O$	59.30	28.63	3.25	0.00
NPX-LEuH-1:1	$Eu(OH)_{2.50}(NO_3)_{0.01}(C_{14}H_{13}O_3)_{0.07}(OH^-)_{0.42}\cdot 0.30H_2O$	78.67	6.42	2.32	0.08
NPX-LEuH-1:1.2	$Eu(OH)_{2.50}(NO_3)_{0.0015}(C_{14}H_{13}O_3)_{0.05}(OH^-)_{0.45}\cdot 0.45H_2O$	71.69	4.04	2.13	0.01

3.2 FT-IR, SEM and thermal analyses of samples.

For NO_3–LEuH (Fig. 2a), the sharp and strong peak at 1384 cm^{-1} is characteristic of the ν_3 vibration mode of uncoordinated NO_3^-.[30] For NPX (Fig. 2b), the band at 3453/3239 cm^{-1} is the characteristic absorption of –OH and the band at 1726 cm^{-1} is the stretching vibration of –C=O. The band at 1609 cm^{-1} and 1456 cm^{-1} are vibration absorptions of benzene ring. The band at 1391 cm^{-1} and 1261 cm^{-1} are ascribed to bend/stretch and stretch/bend vibration of –COOH. 1177 cm^{-1} is due to the absorption of C-O group. The band at 1026 cm^{-1} and 860 cm^{-1} are ascribed to ν_{as} and ν_s vibrations of C–O–C group.[22] In the composites of NPX-LEuH (Fig. 2c-f), the bands at 1551/1558/1549/1540 cm^{-1} and 1410/1406/1391/1389 cm^{-1} are assigned to the ν_{as} and ν_s vibrations of deprotonated $–COO^-$ group. Compared with NPX, the absorption of C=O moves to low frequency due to the interaction between host layers and guest NPX. The bands around 581 cm^{-1} ascribed to Eu–O vibrations also verify the formation of the layered composites.[19]

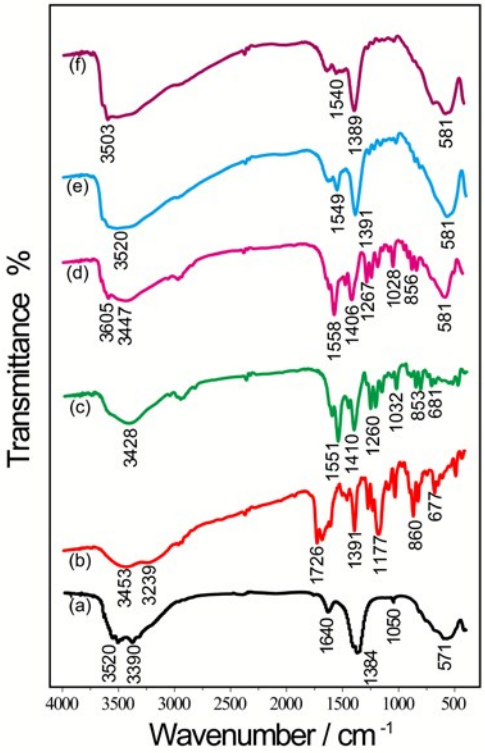

Fig. 2 FT-IR spectra of NO_3-LEuH (a), NPX (b), and composites of NPX-LEuH-1:0.5 (c), NPX-LEuH-1:0.7 (d), NPX-LEuH-1:1 (e), NPX-LEuH-1:1.2 (f).

TG-DTA results indicate the thermal stability after intercalation of organics. Compared with the exothermic peaks at 499°C for NPX (Fig. 3b) related to combustion of organics, the NPX-LEuH-1:0.5 composite (Fig. 3c) shows exothermic peaks at 505 °C. This indicates a slightly heightened thermal stability by 5-6°C. The weight loss of the composite is much higher than the NO_3-LEuH (Fig. 3a) but lower than the NPX (Fig. 3b), indicating the inclusion of organic guests and LEuH layer. Hence, TG-DTA results indicate the composite has better thermal stability in comparison with organics.

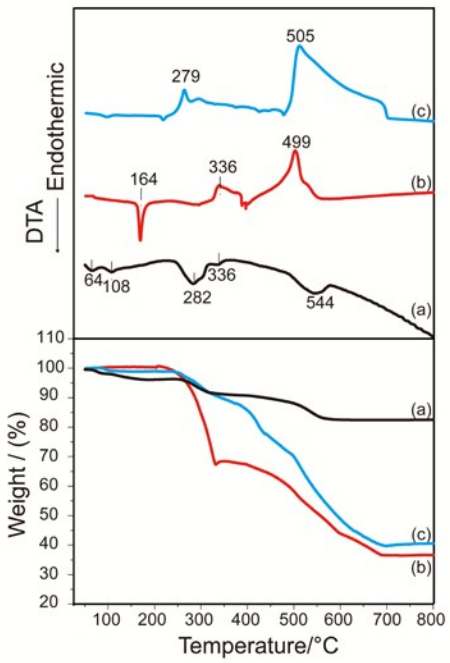

Fig. 3 TG-DTA curves of NO_3-LEuH (a), NPX (b), and NPX-LEuH-1:0.5 composite.

SEM images show the NO_3–LEuH precursor (Fig. 4a,a') is mainly crystallized into elongated hexahedron platelets. The composites (Fig. 4b-e,b'-e') retain the hexagonal morphology and grow into columnar or flower-like aggregates resembling LEuH precursor, as observed in our precious work.[19, 26]

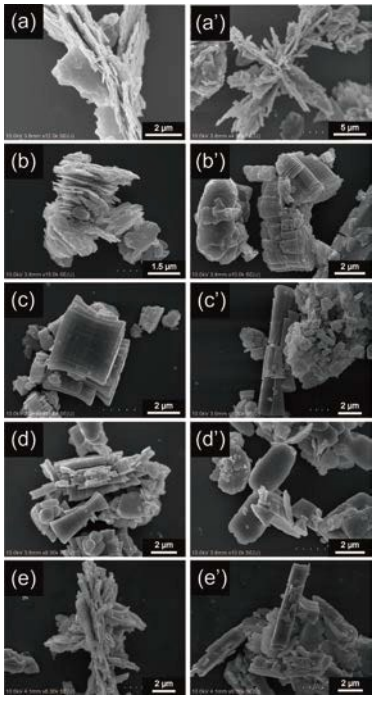

Fig. 4 SEM images of precursor NO_3-LEuH (a, a'), and composites NPX-LEuH-1:0.5 (b, b'), NPX-LEuH-1:0.7 (c,c'), NPX-LEuH-1:1 (d,d'), NPX-LEuH-1:1.2 (e,e').

3.3 Luminescence of NPX-LEuH composites.

For LEuH precursor (Fig. 5a), typical emission peaks observed at 580, 589/595, 613, 654, and 698 nm assigned to $^5D_0$–^7F_J (J = 0, 1, 2, 3, 4) radiative-relaxational transitions of Eu^{3+} are observable. After forming composites, the Eu^{3+} luminescence in NPX-LEuH-1:0.5 composite is markedly enhanced. This may be caused by the efficient energy transfer between intercalated NPX anions and Eu^{3+} centers. For the NPX-LEuH-1:0.7/1/1.2 composites, the Eu^{3+} luminescence intensity show slightly enhancement. This may be interpreted as that the triplet state energy level of organics matches well with the resonant $^5D_0$ energy level of Eu^{3+} for composites with low deprotonation degree and NPX can transfer energy to Eu^{3+} more efficiently in this case.

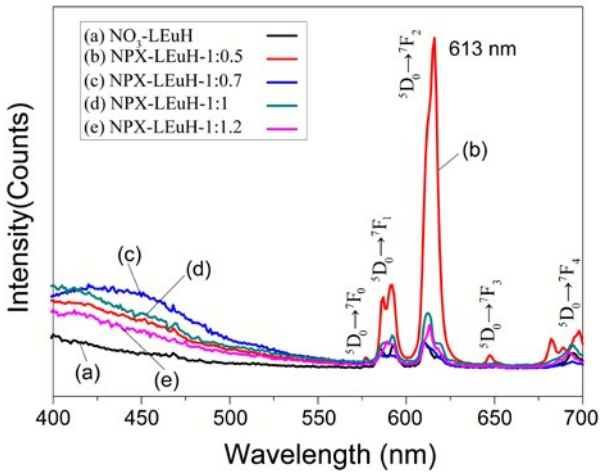

Fig. 5 Emission spectra of NO_3-LEuH (a), and composites NPX-LEuH-1:0.5 (b), NPX-LEuH-1:0.7 (c), NPX-LEuH-1:1 (d), NPX-LEuH-1:1.2 (e).

3.4 The HPLC method validation and the cytotoxic effect

Fig. 6 shows the typical HPLC chromatograms of NPX. Under the condition of detection, the retention time for NPX is approximately 4.4 min. Chromatographic peak of NPX in the standard sample exhibited a sharp and symmetical profile (Fig.6A). Similar peak is observed in the chromatogram obtained in the drug containing sample NPX-LEuH-1:0.5, excluding that the peaks of LEuH appear in approximate 2.3~2.6 min, suggesting the LEuH does not interfere with the measure of NPX (Fig.6B).

To evaluate the cytotoxic effect of NO_3-LEuH, brain glioma U87MG cells, breast cancer MDA-MB-435S cells, murine brain microvascular endothelial cells (BMVECs), and human umbilical vein endothelial cells (HUVECs) are treated with NO_3-LEuH in the range of 0 – 100.0 μg/ml. After incubation for another 48 h, the cytotoxic effect was observed with a sulforhodamine B (SRB) colorimetric assay. The survival ratios are calculated using the following formula:

$$Survival \quad rate\% = \frac{A_{540nm} \ for \ \ treated \ \ cells}{A_{540nm} \ for \ \ control \ \ cells} \times 100\%$$

where $A_{540\ nm}$ represents the average absorbance value.

As is shown in Fig.7, all the cells (except BMVECs) display little cell death even at a high concentration of LEuH, which reveal that the LEuH has low cytotoxic effects on most cells.

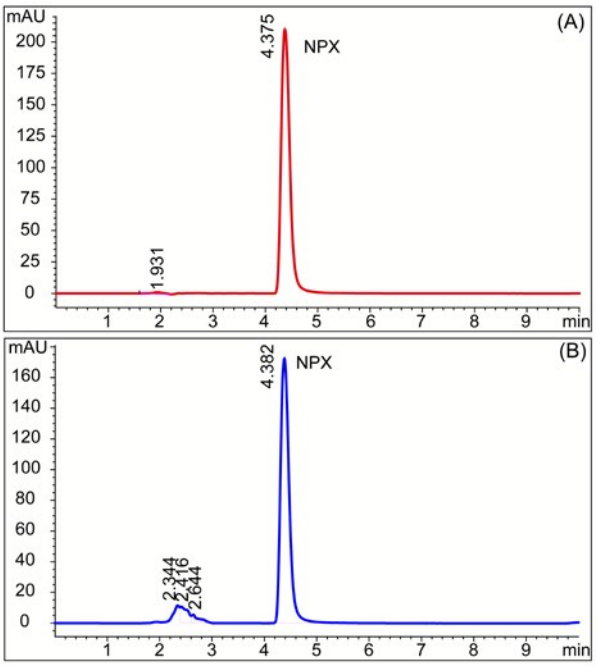

Fig. 6 HPLC chromatograms of NPX under the measuring condition: (A) chromatogram from a standard sample NPX. (B) choromatogram from the drug-containing sample NPX-LEuH-1:0.5.

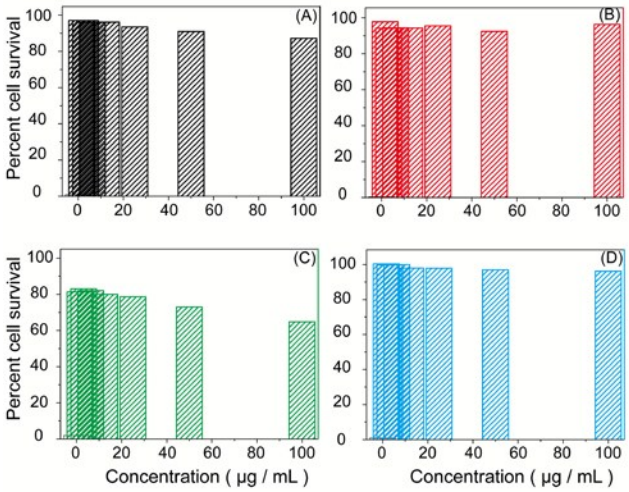

Fig. 7 Cytotoxic effect of NO_3-LEuH on different cells based on cell survival assay. (A) brain glioma U87MG cells. (B) breast cancer MDA-MB-435S cells. (C) murine brain microvascular endothelial cells (BMVECs). (D) human umbilical vein endothelial cells (HUVECs).

3.5 The NPX release of NPX-LEuH nanocomposites.

Fig. 8 shows the UV-vis absorption spectra of NPX-Na in Na_2HPO_4-NaH_2PO_4 buffer solution (pH=6.86), the concentration of the solution is 2×10^{-5} mol·L^{-1}. There exists three main peaks at 288 nm, 317 nm, and 330 nm, and the maximum peak appears at 330 nm. So 330 nm is choosed as UV detection wavelength to measure the standard curve, and the standard curve equation is shown as follows:

$$Conc(mol \cdot L^{-1}) = 7.01\times10^{-6}\,Abs + 2.07\times10^{-7}$$

Where the *Conc* and *Abs* is the concentration and absorbance of the NPX-Na soultion.

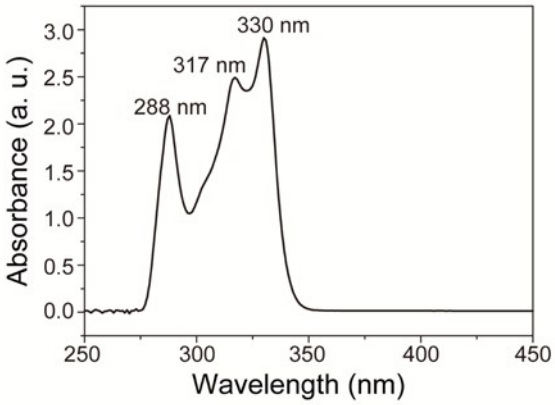

Fig. 8 UV-vis absorption spectra of NPX-Na in Na_2HPO_4-NaH_2PO_4 buffer solution (pH=6.86), the concentration of the solutions is 2×10^{-5} mol·L^{-1}.

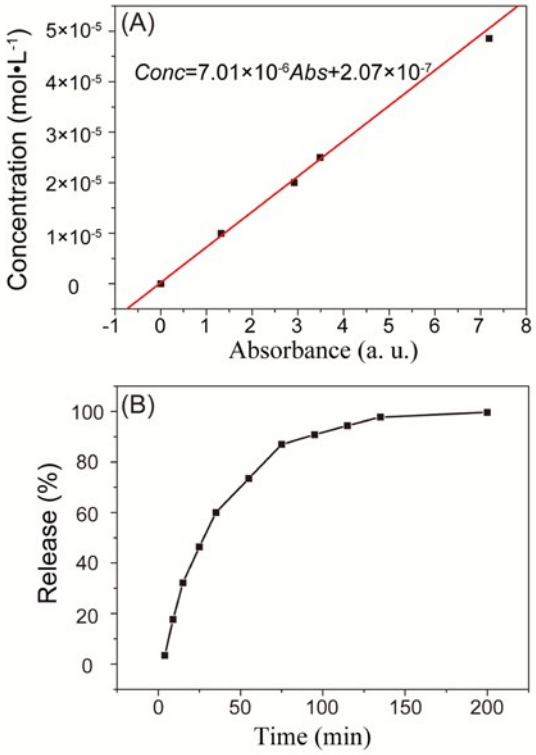

Fig. 9 (A) The standard curve of concentration-absorbance of NPX-Na in Na_2HPO_4-NaH_2PO_4 buffer solution (pH=6.86). (B) Release kinetics of NPX from NPX-LEuH-1:0.5 nanocomposite at pH 6.86 and 37°C.

As is shown in the release profile of NPX from NPX-LEuH-1:0.5 at pH 6.86 and 37°C (Fig. 9), the NPX-LEuH nanocomposite can control the release of NPX. The contact time needed for 91% of the maximum NPX-release amount is 135 min, and the complete release needs about 200 min. The release mechanism can be ascribed to the ion-exchange reaction between NPX and HPO_4^{2-}/$H_2PO_4^-$ in bulk solution. The ion-exchange velocity is fast at beginning and slows down gradually with the exchange reaction. The experimental results indicate that the NPX-LEuH nanocomposite is indeed a potential drug delivery system, which may be attributed to the retricted motion of NPX anions arising from steric effect of LRHs and the electrostatic interaction between NPX anions and positively charged LRHs layers.

4. Conclusions

In summary, the drug naproxen (NPX) is intercalated into layered europium hydroxide (LEuH) to form nanocomposites. Different deprotonation degree leads to NPX-LEuH composites with diverse structure (horizontal and vertical arrangement), and TG-DTA results indicate an elevated thermal stability of organic species after intercalation. Photoluminescence investigation show that the Eu^{3+} luminescence is markedly enhanced for the NPX-LEuH-1:0.5 and the composites with more complete deprotonation (NPX-LEuH-1:0.7/1:1/1:1.2) show slightly luminescence enhancement. This may be ascribed to the well matching of triplet energy level between NPX and Eu^{3+} for NPX-LEuH-1:0.5 composite and NPX can transfer energy to Eu^{3+} more efficiently in this case. The content of naproxen in the intercalation material can be confirmed by HPLC. The cytotoxic effect of LEuH is observed with a sulforhodamine B (SRB) colorimetric assay, which reveal that the LEuH has low cytotoxic effects on most cells. The drug release behavior is studied detailly in Na_2HPO_4-NaH_2PO_4 buffer solution (pH 6.86 and 37°C). The NPX-LEuH composites can control release NPX and the complete release needs about 200 min. The release mechanism can be ascribed to the ion-exchange reaction between NPX and HPO_4^{2-}/$H_2PO_4^-$ in bulk solution. The fabrication of LRHs nanocomposites with drug molecules shows a novel method to

prepare nano-drug delivery system based LRHs integrating drug-loading and fluorescence properties, which have potential applications in the fields of drug detection and delivery system in biologic system.

Acknowledgments.

This work is supported by the Undergraduates Research Training Program (URT: 2016J00103) of Beijing Municipal Education Commission.

Notes and references

† *Department of Chemical Engineering, Beijing Institute of Petrochemical Technology, Beijing 102617, China*

Fax: 86 10 81292133; Tel: 86 10 81292133; E-mail: guqingyang@bipt.edu.cn

1. J.-H. Choy, J.-S. Jung, J.-M. Oh, M. Park, J. Jeong, Y.-K. Kang and O.-J. Han, *Biomaterials*, 2004, **25**, 3059-3064.
2. S. Wang, *Microporous Mesoporous Mater.*, 2009, **117**, 1-9.
3. G. Cavallaro, P. Pierro, F. S. Palumbo, F. Testa, L. Pasqua and R. Aiello, *Drug Delivery*, 2004, **11**, 41-46.
4. Y. Wang, Q. Zhao, N. Han, L. Bai, J. Li, J. Liu, E. Che, L. Hu, Q. Zhang and T. Jiang, *Nanomedicine: NBM*, 2015, **11**, 313-327.
5. I. I. Slowing, J. L. Vivero-Escoto, C.-W. Wu and V. S.-Y. Lin, *Adv. Drug Delivery Rev.*, 2008, **60**, 1278-1288.
6. C.-J. Wang, T.-C. Chen, J.-H. Lin, P.-R. Huang, H.-J. Tsai and C.-S. Chen, *J. Colloid Interface Sci.*, 2015, **440**, 179-188.
7. M. Karimi, N. Solati, M. Amiri, H. Mirshekari, E. Mohamed, M. Taheri, M. Hashemkhani, A. Saeidi, M. A. Estiar and P. Kiani, *Expert Opinion Drug Delivery*, 2015, **12**, 1071-1087.
8. J. K. Oh, R. Drumright, D. J. Siegwart and K. Matyjaszewski, *Prog. Polym. Sci.*, 2008, **33**, 448-477.
9. R. Nigmatullin, P. Thomas, B. Lukasiewicz, H. Puthussery and I. Roy, *J. Chem. Technol. Biotechnol.*, 2015, **90**, 1209-1221.
10. B. Sels, D. De Vos, M. Buntinx, F. Pierard, A. K. Mesmaeker and P. Jacobs, *Nature* 1999, **400**, 855.
11. S. Takagi, D. A. Tryk and H. Inoue, *J. Phys. Chem. B*, 2002, **106**, 5455-5460.
12. K. Zhang, Z. P. Xu, J. Lu, Z. Y. Tang, H. J. Zhao, D. A. Good and M. Q. Wei, *Int. J. Mol. Sci.*, 2014, **15**, 7409-7428.
13. A. I. Khan, L. Lei, A. J. Norquist and D. O'Hare, *Chem. Commun.*, 2001, 2342-2343.
14. M. Z. B. Hussein, Z. Zainal, A. H. Yahaya and D. Wong Vui Foo, *J. Controlled Release*, 2002, **82**, 417-427.
15. F. Geng, R. Ma and T. Sasaki, *Acc. Chem. Res.*, 2010, **43**, 1177-1185.
16. F. Gándara, J. Perles, N. Snejko, M. Iglesias, B. Gómez-Lor, E. Gutiérrez-Puebla and M. Monge, *Angew. Chem. Int. Ed.*, 2006, **45**, 7998-8001.
17. F. Gándara, E. G. Puebla, M. Iglesias, D. M. Proserpio, N. Snejko and M. A. Monge, *Chem. Mater.*, 2009, **21**, 655-661.
18. W. Li, Q. Gu, F. Su, Y. Sun, G. Sun, S. Ma and X. Yang, *Inorg. Chem.*, 2013, **52**, 14010-14017.
19. N. K. Chu, Y. H. Sun, Y. S. Zhao, X. X. Li, G. B. Sun, S. L. Ma and X. J. Yang, *Dalton Trans.*, 2012, **41**, 7409-7414.
20. Q. Gu, F. Su, S. Ma, G. Sun and X. Yang, *Chem. Commun.*, 2015, **51**, 2514-2517.
21. L. Liu, M. Yu, J. Zhang, B. Wang, W. Liu and Y. Tang, *J. Mater. Chem. C*, 2015, **3**, 2326-2333.
22. A. Tabak, N. Yilmaz, E. Eren, B. Caglar, B. Afsin and A. Sarihan, *Chem. Eng. J.*, 2011, **174**, 281-288.
23. G. Bettinetti, M. Sorrenti, A. Negri, M. Setti, P. Mura and F. Melani, *Pharm. Res.*, **16**, 689-694.
24. W.-G. Hou and Z.-L. Jin, *Colloid. Polym. Sci.*, 2007, **285**, 1449-1454.
25. M. Wei, S. Shi, J. Wang, Y. Li and X. Duan, *J. Solid State Chem.*, 2004, **177**, 2534-2541.
26. Q. Y. Gu, N. K. Chu, G. H. Pan, G. B. Sun, S. L. Ma and X. J. Yang, *Eur. J. Inorg. Chem.*, 2014, **3**, 559-566.
27. L. Wang, D. Yan, S. Qin, S. Li, J. Lu, D. G. Evans and X. Duan, *Dalton Trans.*, 2011, **40**, 11781-11787.
28. F. X. Geng, H. Xin, Y. Matsushita, R. Ma, M. Tanaka, F. Izumi, N. Iyi and T. Sasaki, *Chem. Eur. J.*, 2008, **14**, 9255-9260.
29. F. Geng, Y. Matsushita, R. Ma, H. Xin, M. Tanaka, F. Izumi, N. Iyi and T. Sasaki, *J. Am. Chem. Soc.*, 2008, **130**, 16344-16350.
30. Q. Y. Gu, G. H. Pan, T. Ma, G. L. Huang, G. B. Sun, S. L. Ma and X. J. Yang, *Mater. Res. Bull.*, 2014, **53**, 234-239.

Graphical Abstract

Fabrication of nano-drug delivery system based layered rare-earth hydroxides integrating drug-loading and fluorescence properties

Qingyang Gu,* Wen Chen，Fei Duan，Ruijun Ju

Intercalation naproxen (NPX) into LEuH to form nanocomposites with low cytotoxic effect, which can control the release of NPX.